

All-Carbon Molecules: Evidence for the Generation of Cyclo[18]carbon from a Stable Organic Precursor

FRANÇOIS DIEDERICH,* YVES RUBIN, CAROLYN B. KNOBLER, ROBERT L. WHETTEN, KENNETH E. SCHRIVER, KENDALL N. HOUK, YI LI

The unambiguous structural characterization of a single-sized all-carbon molecule requires its chemical synthesis. For cyclo[18]carbon, ab initio calculations predict a relatively stable, cyclic D_{9h} ground state geometry with alternating C-C (1.36 angstroms) and C=C (1.20 angstroms) bonds. The synthesis and x-ray crystal structure of a direct precursor to C_{18} are described. The analysis of laser flash heating experiments on this precursor by time-of-flight mass spectroscopy shows a sequence of retro-Diels-Alder reactions leading to C_{18} as the predominant fragmentation pattern. Structural evidence is provided for the generation of an all-carbon molecule from a well-characterized organic precursor.

ALL-CARBON MOLECULES C_n have fascinated researchers in a number of fields (1) and have recently become the subject of an increasing number of experimental and theoretical studies (1-5). Studies of all-carbon molecules of various sizes are intended to show how the properties of carbon evolve as its structure changes from molecular to bulk material. The relevance of all-carbon molecules in combustion processes has been demonstrated (6), and they are believed to be present in the interstellar dust (7). Laser vaporization of graphite can be used to produce supersonic beams containing compounds ranging from C_2 to $>C_{60}$ that can be studied with a variety of molecular beam techniques (5, 8-11). For the smaller molecules C_2 through C_9 , linear chain structures, and, for compounds as small as C_3 , cyclic structures also have been discussed (3). The theoretical consensus is that the larger molecules C_{10} through C_{29} should have monocyclic ring structures, and experiments have been interpreted consistently in this way (12-16). Special stability is predicted for the neutral cycles with $4n + 2$ atoms that are aromatic closed-shell species, such as C_{14} , C_{18} , or C_{22} . Carbon molecules in the range from C_{30} to C_{40} are, by comparison, very reactive (16). Above C_{40} , more stable even-numbered molecules begin to dominate, and closed spheroidal structures have been advanced (2, 4, 8). The exceptional stability of C_{60} has been explained with

the highly symmetrical truncated icosahedral geometry characteristic of a soccer ball (2).

Chemical synthesis of a single-sized all-carbon molecule is required for the unambiguous determination of its chemistry and physics. However, no polyatomic carbon molecules have yet been prepared by a total synthesis. We present a synthetic approach to C_{18} (1), generated from a stable, well-characterized precursor (Fig. 1). Compound 1 belongs to the class of monocyclic molecules that we systematically name as the cyclo[n]carbons. As in the [n]annulenes, n defines the number of carbon atoms that are

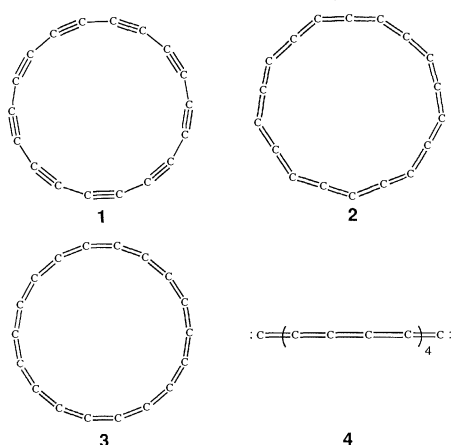


Fig. 1. Theoretical results for C_{18} compounds. Compound 1 (D_{9h}) has C-C-C angles of 160° and C-C and C=C bond lengths of 1.362 and 1.199 Å, respectively. Compound 2 (D_{9h}) has alternating C-C-C angles of 170.4° and 149.6° , and a C=C bond length of 1.271 Å. Compound 3 (D_{18h}) has C-C-C angles of 160° and a C=C bond length of 1.265 Å. Compound 4 ($D_{\infty h}$) has C=C bond lengths that vary from 1.258 to 1.281 Å.

Table 1. Relative energies (kilocalories per mole) of optimized cyclo[18]carbon structures. For bond lengths and bond angles, see captions to Fig. 1. The AM1 method (Austin Model 1) is semi-empirical (32); STO-3G is a minimal basis set of Gaussian functions; and 3-21G is a split-valence basis set (33).

Method	Compound			
	1	2	3	4
AM1	0.0	53.9	56.3	119.9
Ab initio (STO-3G)	0.0	85.8	105.0	177.9
Ab initio (3-21G)	0.0	37.6	53.8	107.4

connected to form the monocyclic ring structure. Cyclo[18]carbon could have a distinctive form of aromaticity since it possesses two perpendicular systems of π -orbitals, one in-plane and one out-of-plane, with $4n + 2$ π -electrons each. Both can stabilize the molecule.

The choice of cyclo[18]carbon as a prime synthetic target was based on evaluation of its chemical stability and on the availability of a suitable synthetic sequence. The structural details of C_{18} were studied by both semi-empirical and ab initio molecular orbital calculations (17). Geometry optimization was performed within the given symmetry constraints at the Hartree-Fock level of theory. The energies (Table 1) of the optimized planar monocyclic (1 to 3) and singlet acyclic (4) structures reveal that the monocyclic structures are more stable than the singlet acyclic structure. Even for cyclo[n]carbons

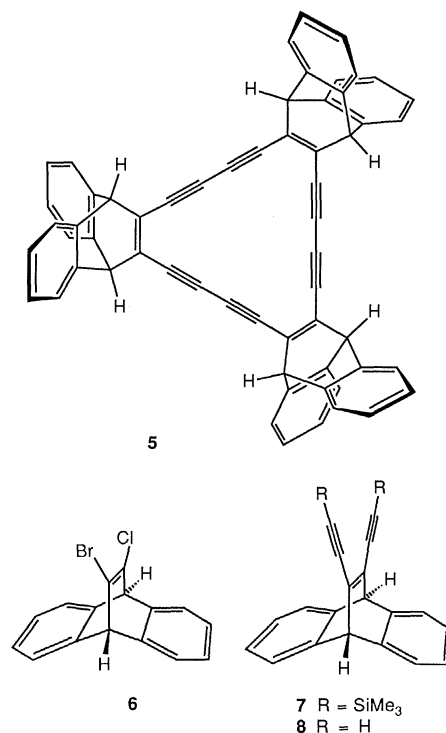


Fig. 2. Compounds 5 through 8.

Department of Chemistry and Biochemistry, University of California, Los Angeles, CA 90024.

*To whom correspondence should be addressed.

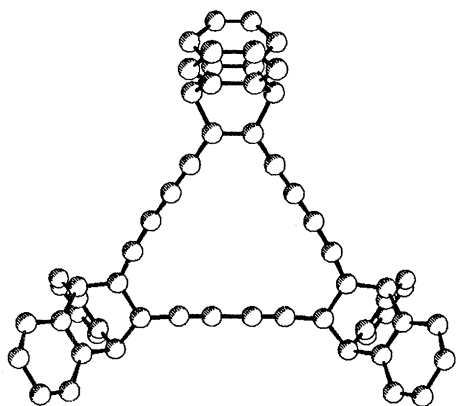
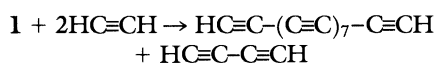


Fig. 3. X-ray crystal structure of the [18]annulene **5**.

with $n = 4, 6, 8,$ and 10 , the cyclic singlet is found to be more stable than the acyclic ground-state triplet (18), and the same should be true for C_{18} . The higher stability of a monocyclic structure for cyclo[18]carbon had been predicted by semi-empirical calculations (10, 13, 14). The cyclic D_{9h} structure **1** with alternating bonds is more stable than the D_{9h} structure **2** or the D_{18h} structure **3**, which have uniform bond lengths. The D_{9h} structure **1** is an energy minimum on the potential energy surface as characterized by the calculations of harmonic vibrational frequencies, but structures **2** and **3** are not. Optimizations of structures with lower symmetry led always to structure **1**. According to group equivalents (19), the alternating (acetylenic) structure **1** should be at least 60 kcal/mol more stable than the nonalternating **2**, and the aromaticity-induced driving force for bond length equalization should be less than this value.

Strain in the monocyclic structures **1**, **2**, and **3** results mainly from the distortion of bond angles from the ideal value, 180° , to $\sim 160^\circ$. This distortion of an acetylenic or allenic angle requires about 4 kcal/mol, leading to a predicted total strain of 72 kcal/mol. We also assessed the strain energy of structure **1** computationally. The energy change for the following reaction is 76 kcal/mol, which is far less than the energy of about 130 kcal/mol (19) required to cleave a C–C single bond joining two acetylenes.



Compound **5** was chosen as the direct precursor to **1**, since it contains the macrocyclic framework of **1** and can lose three anthracenes in a retro-Diels-Alder reaction under flash vacuum pyrolysis conditions to give the cyclo[18]carbon molecule. With the retro-Diels-Alder reaction, a well-established route for the preparation of strained acetylenes from bridged ethenoanthracenes was chosen to interrelate structurally the

formed C_{18} with a fully characterized chemical precursor (20). In the synthesis of **5**, compound **7** [melting point (mp) 209° to 210°C , 87% yield] was obtained by alkynylation of **6** (21) with trimethylsilylacetylene in *n*-butylamine in the presence of $\text{Pd}(\text{PPh}_3)_4$ and CuI (22) (Fig. 2). Deprotection of **7** in methanol with KOH gave **8** as very unstable crystals [mp $> 30^\circ\text{C}$, decomposition (dec.); 98% yield]. Oxidative coupling of **8** under Eglinton-Glaser conditions (23) afforded the cyclic trimer **5** as the only product in 25% yield. Compound **5**, according to ^1H nuclear magnetic resonance (NMR) criteria (24), is aromatic and is among the most stable [18]annulenes ever reported (25). The parent compound 1,3,5,7,9,13,15-hexadehydro[18]annulene is unstable in the solid state and explodes at $\sim 85^\circ\text{C}$ (26), whereas compound **5** can be heated to 250°C in the solid state (sealed tube) without decomposition and is perfectly stable to air.

The structure of **5** was confirmed by x-ray diffraction analysis on crystals obtained by recrystallization from boiling pyridine (27). The D_{3h} geometry of **5** in the crystal is shown in Fig. 3, and it is apparent that the steric shielding provided by the six benzene rings is at the origin of the unusual stability with respect to bimolecular reactions and polymerization of this planar [18]annulene perimeter.

We have carried out a series of microsecond laser flash-heating experiments to confirm that the retro-Diels-Alder elimination sequence would be the predominant fragmentation pattern of **5**. In these experiments, we used 10^{-8} -s ultraviolet light pulses to heat a thin film of **5** coated onto a metal rod, which in turn was mounted in vacuum within a pulsed He jet nozzle source and molecular beam chamber (28). Under gentle flash-heating conditions [$15 \text{ mJ}/\text{cm}^2$ or $\Delta T \approx 400 \text{ K}$ estimated transient temperature jump (29)], the parent molecule **5** is the dominant desorbed product, as detected by resonant two-photon ionization mass spectrometry of the He-cooled desorption cloud. A time-of-flight mass spectrum under stronger heating conditions ($30 \text{ mJ}/\text{cm}^2$, $\Delta T \approx 800 \text{ K}$) and identical ionization-detection conditions (Fig. 4a) shows the parent and fragments resulting from the loss of one or two anthracenes. Very little indication of competing decomposition pathways is evidenced, consistent with the picture that the retro-Diels-Alder reaction channel is dominant. At even stronger heating conditions ($> 40 \text{ mJ}/\text{cm}^2$, $\Delta T \geq 1000 \text{ K}$), additional fragmentation occurs (Fig. 4b), and the fragment corresponding to C_{18} (**1**) becomes visible. Although we have associated these effects with the laser heating condi-

tions in the experiment, some fragmentation following ionization cannot be entirely ruled out. The presence of only a weak peak originating from neutral C_{18} (Fig. 4b) is consistent with the reported absence of resonant two-photon ionization resonances in experiments on polydisperse carbon cluster beams generated by graphite vaporization

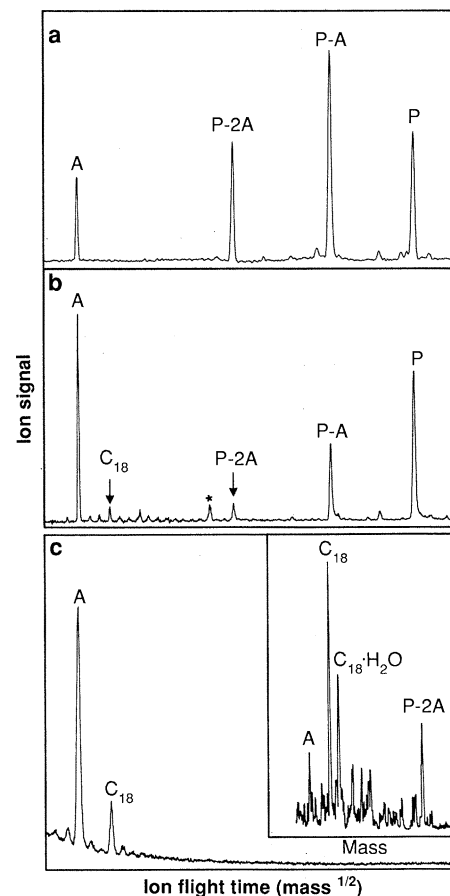


Fig. 4. Time-of-flight mass spectra of the neutral desorbed products of laser flash-heating of a thin film of **5** coated on a tantalum rod. (a) Desorption was by a $30 \text{ mJ}/\text{cm}^2$ pulse from a XeCl laser over a 0.01-cm^2 irradiated area, coincident with a He pulse through the nozzle (stagnant pressure = 7 atm). The products were ionized by a $5 \text{ mJ}/\text{cm}^2$ pulse from an ArF laser (193 nm) in the ion-source region of the spectrometer. The identified peaks are coded P (parent **5**) and A (anthracene, $\text{C}_{14}\text{H}_{10}$). (b) Same as (a), except that the desorption laser intensity was increased to $\geq 40 \text{ mJ}/\text{cm}^2$. The asterisk marks a mass peak due to contamination in the spectrometer. (c) Time-of-flight mass spectrum, generated by simultaneous desorption and ionization of a thin film of **5** coated on a quartz plate in the ion-source region of the mass spectrometer. A single XeCl laser pulse of $20 \text{ mJ}/\text{cm}^2$ accomplishes both heating desorption and subsequent ionization. (Inset) Quadrupole mass spectrum of ions generated by simultaneous desorption and ionization of a thin film of **5** coated on a tantalum rod followed by cooling in a He pulse as described for Fig. 2. Again, a single XeCl laser pulse of $\sim 60 \text{ mJ}/\text{cm}^2$ was used for both heating-desorption and ionization. The peak of $\text{C}_{18}\cdot\text{H}_2\text{O}$ results from contamination during the preparation procedure.

(30). A range of experiments revealed a complicated bimolecular chemistry at higher desorption laser fluences and is the subject of continuing analysis.

That C₁₈ (1) can be formed with high efficiency through this process is indicated by two other experiments: (i) detection of the He-cooled ions produced directly by ultraviolet radiation during the evaporation process, and (ii) same as (i) but without He cooling gas (31). In the latter case (Fig. 4c), both anthracene and C₁₈⁺ ions are dominant. In the former case (Fig. 4c, inset), the C₁₈⁺ ion (and C₁₈⁺ · H₂O contaminant ion) is actually dominant over a range of heating and ionization conditions. We take these results as strong evidence that C₁₈ is the terminal product of the dominant fragmentation pathway. Besides supporting the precursor status of compound 5 in chemical synthesis, these results also allow one to envisage spectroscopic experiments on the cooled C₁₈ molecules in molecular beams. It should be possible to isolate preparative quantities of cyclo[18]carbon 1 from flash vacuum pyrolysis reactions (32).

REFERENCES AND NOTES

- E. A. Rohlffing, D. M. Cox, A. Kaldor, *J. Chem. Phys.* **81**, 3322 (1984); see historical discussion within.
- R. F. Curl and R. E. Smalley, *Science* **242**, 1017 (1988).
- W. L. Brown *et al.*, *ibid.* **235**, 860 (1987).
- H. W. Kroto, *Nature* **329**, 529 (1987); S. Iijima, *J. Phys. Chem.* **91**, 3466 (1987).
- D. C. Parent and S. W. McElvany, *J. Am. Chem. Soc.* **111**, 2393 (1989).
- P. Gerhardt, S. Löffler, K. H. Homann, *Chem. Phys. Lett.* **137**, 306 (1987).
- A. E. Douglas, *Nature* **269**, 130 (1977).
- Q. L. Zhang *et al.*, *J. Phys. Chem.* **90**, 525 (1986); S. H. Yang, C. L. Pettiette, J. Conceicao, O. Chesnovsky, R. E. Smalley, *Chem. Phys. Lett.* **139**, 233 (1987); J. R. Heath *et al.*, *J. Am. Chem. Soc.* **109**, 359 (1987); S. C. O'Brien, J. R. Heath, R. F. Curl, R. E. Smalley, *J. Chem. Phys.* **88**, 220 (1988).
- L. A. Bloomfield, M. E. Geusic, R. R. Freeman, W. L. Brown, *Chem. Phys. Lett.* **121**, 33 (1985); M. E. Geusic, M. F. Jarrold, T. J. McIlrath, R. R. Freeman, W. L. Brown, *J. Chem. Phys.* **86**, 3862 (1987).
- J. Bernholc and J. C. Phillips, *J. Chem. Phys.* **85**, 3258 (1986).
- H. Y. So and C. L. Wilkins, *J. Phys. Chem.* **93**, 1184 (1989).
- E. Dörnenburg, H. Hintenberger, J. Franzen, *Z. Naturforsch.* **16A**, 532 (1961).
- K. S. Pitzer and E. Clementi, *J. Am. Chem. Soc.* **81**, 4477 (1959).
- R. Hoffmann, *Tetrahedron* **22**, 521 (1966).
- N. Fürstenau and F. Hillenkamp, *Int. J. Mass Spectrom.* **37**, 135 (1981).
- S. Yang *et al.*, *Chem. Phys. Lett.* **144**, 431 (1988).
- M. Frisch *et al.*, GAUSSIAN 86, Carnegie-Mellon University, Pittsburgh, PA, 1986.
- K. Raghavachari and J. S. Binkley, *J. Chem. Phys.* **87**, 2191 (1987), and references therein.
- S. W. Benson, *Thermochemical Kinetics* (Wiley, New York, 1968).
- M.-C. Lasne and J.-L. Ripoll, *Synthesis* **1985**, 121 (1985).
- H. Hart, S. Shamouilian, Y. Takehira, *J. Org. Chem.* **46**, 4427 (1981).
- S. Takahashi, Y. Kuroyama, K. Sonogashira, N. Hagihara, *Synthesis* **1980**, 627; W. B. Austin, N.

23. O. M. Behr, G. Eglinton, A. R. Galbraith, R. A. Raphael, *J. Chem. Soc.* **1960**, 3614 (1960).
24. Characterization of 5: mp > 300°C (dec., sealed tube); infrared spectrum (KBr) ν 2160 cm⁻¹. Ultraviolet spectrum (CH₂Cl₂), wavelength λ 243 nm shoulder (sh) (extinction coefficient ϵ 30,600 liter per mole per centimeter), 248 sh (28,700), 264 sh (13,500), 281 (11,500), 318 sh (11,500), 359 sh (45,000), 375 (87,600), 404 sh (8,800), 420 (17,700), 432 (21,000), 453 sh (960). ¹H NMR (360 MHz, CDCl₃) δ 5.89 (s, 6 H), 7.03 (dd, J = 5.3 and 3.2 Hz, 12 H), 7.50 (dd, J = 5.3 and 3.2 Hz, 12 H); ¹³C NMR (90.6 MHz, CDCl₃) δ 56.4, 86.2, 88.7, 124.0, 125.6, 140.0, 144.1; mass spectrum (fast atom bombardment, *m*-nitrobenzyl alcohol): m/z (relative intensity) 751 (MH⁺, 100%), 750 (M⁺, 73%), 573 (MH⁺ - 178 (anthracene), 12%), 572 (M⁺ - 178, 39%). The diatropicity of 5 is supported by the ¹H NMR data. The bridgehead methine protons in 5 are deshielded by 0.75 ppm through the diamagnetic ring current of the 18 π -electron system when compared to the methine protons of 8 (5.14 ppm).
25. E. Vogel, W. Hass, B. Knipp, J. Lex, H. Schmickler, *Angew. Chem. Int. Ed. Engl.* **27**, 408 (1988).
26. W. H. Okamura and F. Sondheimer, *J. Am. Chem. Soc.* **89**, 5991 (1967); H. P. Figey and M. Gelbcke, *Tetrahedron Lett.* **1970**, 5139.
27. X-ray crystal data of 5 (C₆₀H₃₀); M_r = 750.3; orthorhombic; space group = *Pnma*; Z = 4; a (Å) = 8.422 (2); b (Å) = 21.927 (7); c (Å) = 28.851 (8); V = 4966 Å³; D_c (g cm⁻³) = 1.07; a total of 938 reflections with $I > 3\sigma I$. The details of the molecular and crystal structure will be published elsewhere; in the meantime, they are available upon request.
28. J. Grotemeyer, U. Boesl, K. Walter, E. W. Schlag, *Org. Mass. Spectrom.* **21**, 645 (1986).
29. The transient temperature jump (ΔT) at the surface was calculated by using the measured extinction coefficient ϵ (309 nm) = 1.1×10^4 liter mol⁻¹ cm⁻¹, and the density and heat capacity of the solid.
30. D. M. Cox, K. C. Reichmann, A. Kaldor, *J. Chem. Phys.* **88**, 1588 (1988).
31. V. S. Antonov, V. S. Letokhov, A. N. Shibanov, *Appl. Phys.* **25**, 71 (1981).
32. M. J. S. Dewar, E. G. Zoebisch, E. F. Healy, J. J. P. Stewart, *J. Am. Chem. Soc.* **107**, 3902 (1985).
33. W. J. Hehre, L. Radom, P. v. R. Schleyer, J. A. Pople, *Ab Initio Molecular Orbital Theory* (Wiley, New York, 1986).
34. Supported by the Petroleum Research Fund of the ACS (F.D. and Y.R.), by NSF (K.N.H. and Y.L.), and by a NSF Presidential Young Investigator Award and a Sloan Research Fellowship to R.L.W. (R.L.W. and K.E.S.).

18 May 1989; accepted 10 July 1989

Origin of Ancient Potash Evaporites: Clues from the Modern Nonmarine Qaidam Basin of Western China

TIM K. LOWENSTEIN, RONALD J. SPENCER, ZHANG PENGXI

Modern potash salt deposits and associated brines of the Qaidam Basin, western China, demonstrate that some anomalous marine evaporites may have formed from nonmarine brines instead of seawater. Qaidam Basin brines are derived from meteoric river inflow mixed with small amounts of CaCl spring inflow similar in composition to many saline formation waters and hydrothermal brines. Evaporation of spring-enriched inflow yields a predicted mineral sequence including carnallite, bischofite, and tachyhydrite that is identical to several anomalous marine evaporites. Other mixtures of river and spring inflow produce the salt assemblage expected from evaporation of seawater.

EVAPORITES ARE SEDIMENTARY rocks that have formed by precipitation from waters at the earth's surface. Ancient evaporites have been used to track the chemistry of ancient surface waters, especially seawater (1, 2). Study of marine evaporites has led to the general, but not unanimous, consensus that the major element chemistry of seawater has not changed significantly during the Phanerozoic [the last ~600 million years (2, 3)]. One major problem, however, is that ancient evaporites containing soluble potash salts fail to match the mineralogical sequences predicted in the

evaporation of modern seawater. For example, more than half of 50 well-known Phanerozoic potash-bearing evaporites have been called "unusual" or "MgSO₄-deficient" marine evaporites because they are missing MgSO₄ salts that are characteristic of a normal seawater evaporation sequence (1, 4, 5). The discrepancy between predicted versus observed potash-bearing mineral sequences has been attributed either to departures of the parent waters from seawater composition or to diagenetic alteration of the original marine mineral sequence (1, 2, 4, 6, 7).

The origin of ancient potash evaporites, in terms of parent waters (seawater versus nonmarine inflow), depositional environments (deep versus shallow waters), and timing of formation (primary precipitates versus diagenetic alteration products) remains controversial largely because no modern potash-bearing basins have been de-

T. K. Lowenstein, Department of Geological Sciences and Environmental Studies, State University of New York at Binghamton, Binghamton, NY 13901.

R. J. Spencer, Department of Geology and Geophysics, University of Calgary, Calgary, Alberta T2N 1N4 Canada.

Zhang Pengxi, Qinghai Institute of Salt Lakes, Academia Sinica, Xining, Qinghai Province, People's Republic of China.